

1

DTIC FILE COPY

AD-A190 143

WIND-GENERATED NOISE MODELING

DTIC
ELECTE
FEB 10 1988
S D

DISTRIBUTION STATEMENT A
Approved for public release
Distribution Unlimited



ATLANTA • ANN ARBOR • BOSTON • CHICAGO • CLEVELAND • DENVER • HUNTSVILLE • LA JOLLA
LITTLE ROCK • LOS ANGELES • SAN FRANCISCO • SANTA BARBARA • TUCSON • WASHINGTON

88 2 05 047

WIND-GENERATED NOISE MODELING



Accession For	
NTIS CRA&I	<input checked="" type="checkbox"/>
DTIC TAB	<input type="checkbox"/>
Unannounced	<input type="checkbox"/>
Justification	
By <i>per form 50</i>	
Distribution	
Availability Codes	
Dist	Avail and/or
A-1	



ATLANTA • ANN ARBOR • BOSTON • CHICAGO • CLEVELAND • DENVER • HUNTSVILLE • LA JOLLA
 LITTLE ROCK • LOS ANGELES • SAN FRANCISCO • SANTA BARBARA • TUCSON • WASHINGTON

WIND-GENERATED NOISE MODELING

April 1981

Prepared by:

James H. Wilson
Ocean Acoustics Division.

Prepared for:

Dr. R.R. Goodman
Associate Editor, Underwater Sound
The Journal of Acoustical Society of America
Director, Naval Ocean Research and Development Activity
Bay St. Louis, MS 39529

SCIENCE APPLICATIONS, INC.

P.O. Box 1303
1710 Goodridge Drive
McLean, Virginia 22102
(703) 821-4300



TABLE OF CONTENTS

	<u>Page</u>
1.0 INTRODUCTION.....	1
2.0 WIND-GENERATED SOURCE LEVEL DENSITY.....	3
3.0 DEVELOPMENT OF WIND-GENERATED NOISE MODEL.....	9
4.0 MODEL DATA COMPARISON.....	11
5.0 CONCLUSIONS.....	15



LIST OF FIGURES

	<u>Page</u>
Figure 1: Wind-Generated Noise Level Curves.....	4
Figure 2: Model/Data Comparison - 10 Day Averages.....	13
Figure 3: Model/Data Comparison at 250 Hz - Time Series.....	14

LIST OF TABLES

Table I: Wind-Generated Source Level Densities for Dipole Radiation Pattern.....	6
--	---



ACKNOWLEDGMENTS

The author expresses a special thanks to C. W. Spofford of Science Applications, Inc. who is responsible for the contents of the Appendix and who gave the author many useful ideas in the development of the model. The author acknowledges the software development and very helpful suggestions of Ken Osborne, Richard Sequig, and Jim Crouch of Ocean Data Systems, Inc. of San Diego. Without their dedicated efforts these analyses would not be possible. The author is grateful to the Naval Ocean Research and Development Activity - Code 520 for sponsoring this work.

ABSTRACT

The Wilson Wind-Generated Source Level Densities and the ASTRAL propagation loss model are combined to form a wind-generated noise model. The model treats storms as a geographically distributed source and is capable of modeling both distant and local storm noise. Model estimates are compared with omnidirectional measurements from the northeastern Pacific Ocean at 5 frequencies and 3 receiver depths. The results are very good and indicate the necessity of modeling both shipping and wind-generated noise in comparisons with measured data.

1.0 INTRODUCTION

An ambient noise model has three components. First, a geographical distribution of the source of noise (e.g., shipping, wind, etc.) must be specified along with the geographical location and depth of the receiver. Second, the source level, usually specified at some reference distance from the source, and source depth and directivity pattern must be specified. Third, an accurate propagation loss model must be applied between the source distribution and receiver in order to estimate ambient noise levels at the receiver site. The now familiar Wenz¹ curves are not an ambient noise model in this sense. They are noise levels representative of deep water ocean basins. Recent acoustic and oceanographic at-sea measurements made under the sponsorship of the Naval Oceanographic Research and Development Activity have shown the highly variable nature of ambient noise level as a function of time and source/receiver location. One set of ambient noise level curves, while a valuable reference, does not provide the real time ambient noise input that is needed for the optimization of performance of current tactical and surveillance sonar systems. The wind-noise model described in this paper does provide a dynamic, real time estimation of noise due to storms at sea.

In the author's opinion, there are three significant applications of this type of wind-noise model. First, at any given time the model can identify high noise areas and directions where search for signals of interest will be unsuccessful with high probability. Thus, sonar system

resources can be allocated accordingly. Conversely, the model can estimate where and in what directions the noise level due to storms is low so that mobile sonar systems can be placed in the optimum location, depth, and heading to maximize probability of detection of signals of interest. Second, the model can forecast noise levels up to 3 days in the future if the storm path and intensity can be forecasted accurately. This can be used to estimate what the optimum sonar system location and heading will be in the future, or what sonar system resources will be necessary to search, localize, and maintain contact with a signal of interest. Third, if storm noise can be accurately modeled, there is a possibility of subtracting the noise from sonar system measurements to improve system performance. This as yet, has not been demonstrated and will be the subject of further research.

In the frequency range of interest for this model, 10 to 1000 Hz, shipping and wind/storm noise are the major components of the ambient noise field. As described above, wind noise will be modeled from real time wind speed distributions over the ocean surface. In order to evaluate the wind noise model with measured data, shipping needs to be modeled also because both wind and shipping contribute to the measured data. Historical or RMS² shipping densities will be used in the model, because real time shipping densities are not currently available as model inputs. The model output will consist of a wind noise estimate based on dynamic wind speed distributions and a shipping noise estimate based on historical shipping densities that are constant in time.

The wind-generated noise source characteristics are described in the following sections. Details of the wind noise model development are given in Section 3.0. Model/data comparisons are described in Section 4.0 for data collected in the northeastern Pacific Ocean in September 1973.

2.0 WIND-GENERATED SOURCE LEVEL DENSITY

The source level densities of wind-generated noise are shown as a function of frequency and wind speed in Figure 1. These curves are the result of analytical studies of the physical mechanisms of wind-generated noise from 5 to 1000 Hz performed by the author.^{3,4} Deep ocean measurements by Wittenborn and Shooter⁵ and Morris⁶ compare favorably with the results shown in Figure 1.

In deriving the source level density shown in Figure 1, great care was taken to address the difference between noise level and source level. In order to validate wind-generated noise source levels with measured noise levels, only a very select set of measured data can be considered. In the Appendix, it is shown⁷ that source level and noise level are related by a constant factor only when the noise measurements are taken well below critical depth near a region with a poor reflecting bottom where only the noise from the near vertical sea surface above the hydrophone is measured. In this case, the relationship between source level and noise level for a dipole radiation pattern is given by

$$NL(f,U) = \pi SL(f,U) \quad (1)$$

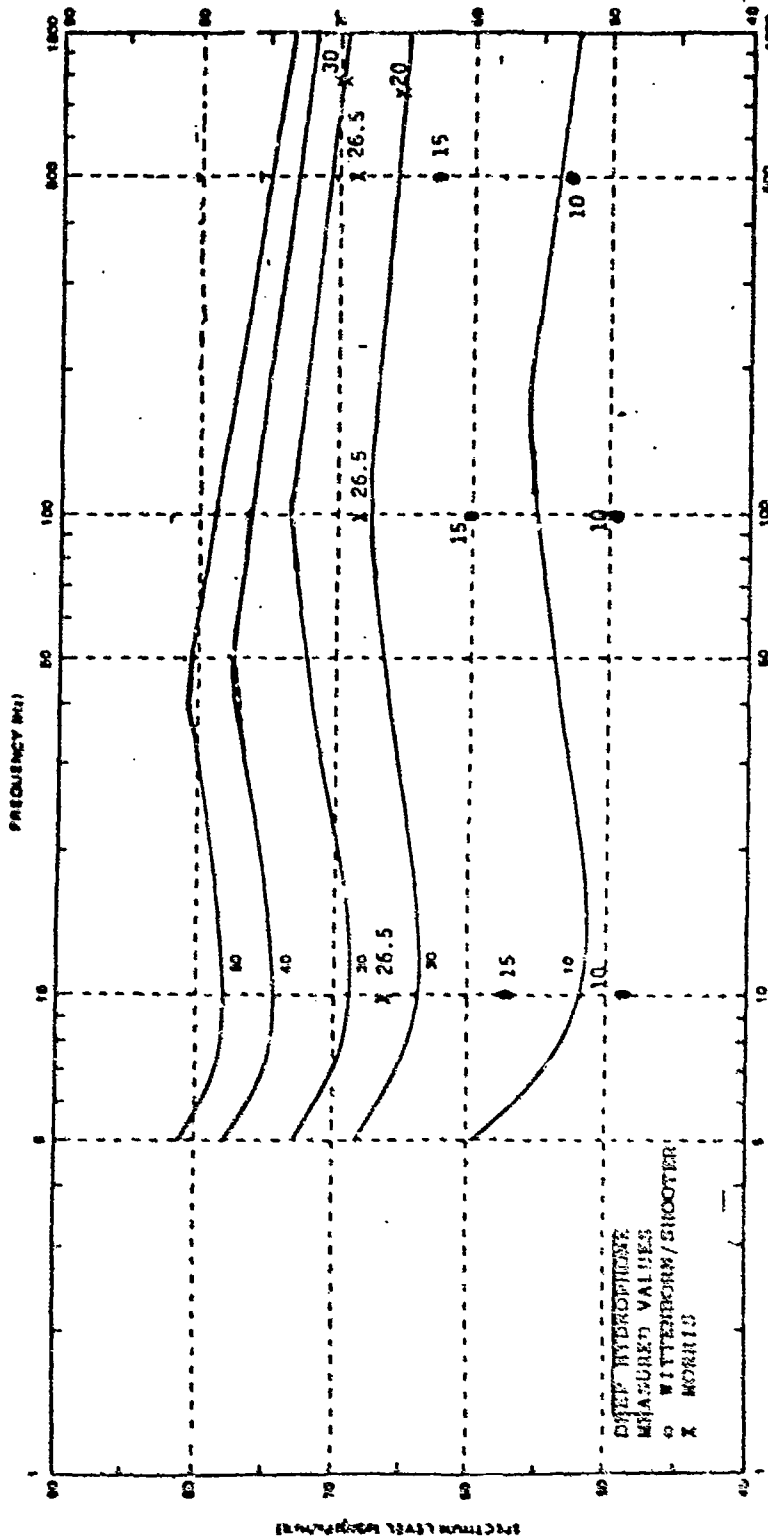


Figure 1. Wind-Generated Noise Level Curves

where f is frequency in Hz and U is wind speed in knots.

In most measured noise data, where the hydrophone is above the critical depth, noise from distant sources becomes important and the frequency dependence of the transmission loss and bottom interaction make it impossible to relate noise level and source level by the simple relation given in Equation (1).

Acoustic Data Capsule (ACODAC) data from the northeastern Pacific analyzed by Wittenborn and Shooter⁵ and FLIP data from the same area analyzed by Morris⁶ were used to validate the analytical results shown in Figure 1. The measured data and analytically derived levels compare favorably. However, more of these near bottom measurements are needed for a wider range of wind speeds and frequencies, since not all frequencies and wind speed intervals were covered by the measured data.

Figure 1 shows noise level values as a function of frequency and wind speed and the corresponding source level values can be derived by using Equation (1) (i.e., divide the noise level value shown in Figure 1 by π). Table I lists the source level values derived from Figure 1 at frequencies selected for input to the model. Linear interpolation between the values shown in Table I is used in the model for frequencies and wind speeds not listed in Table I.

Table I
 WIND-GENERATED SOURCE LEVEL DENSITIES (dB/ μ Pa/Hz^{1/2})
 FOR DIPOLE RADIATION PATTERN

WIND SPEED (Knots)	Frequency (Hz)									
	5	7.5	10	20	50	100	500	1000		
10	55.2	49.0	47.0	47.0	49.0	50.0	49.0	48.0		
15	60.0	56.0	53.4	53.4	55.4	57.2	56.2	56.2		
20	63.1	60.0	59.0	59.5	61.5	62.7	61.7	61.7		
25	66.5	63.5	62.0	62.9	64.0	66.1	63.7	63.7		
30	68.0	65.0	64.4	65.0	68.1	69.0	66.5	65.0		
35	70.5	67.5	66.8	68.5	70.9	70.0	68.6	67.1		
40	73.0	70.0	69.5	70.5	72.0	71.5	69.5	68.0		
45	74.9	71.9	71.4	72.4	72.5	72.7	70.2	68.7		
50	76.0	73.0	73.0	74.0	75.0	73.5	70.9	69.4		
60	78.0	75.0	75.0	76.0	76.2	74.7	72.3	70.6		
70	80.5	77.5	77.3	79.5	77.2	75.7	73.3	71.6		
80	83.0	80.0	80.0	81.5	78.1	76.6	74.2	72.5		
90	84.9	81.9	81.9	82.0	79.9	77.4	75.0	73.3		

2.1 CHARACTERISTICS OF THE WIND-GENERATED NOISE SOURCE

Analyses of the physical mechanisms of wind-generated noise indicate that turbulence pressure fluctuations in the atmosphere near the ocean surface was the dominant physical mechanism from 10 to 80 Hz, while wave-wave interaction was the dominant physical mechanism from 5 to 10 Hz and the impact of ocean spray streaks and whitecaps with the ocean surface was the dominant physical mechanism at higher frequencies from 80 to 1000 Hz. All of the above physical mechanisms had a dipole radiation pattern associated with them. The exact frequency interval over which a particular mechanism is dominant is highly wind speed dependent and the above intervals are only rough approximations.

The wind speed dependence of the wind-generated source levels was significantly different at low and high frequencies. From 5 to 80 Hz, the wind speed dependence of the analytically derived source levels and relevant measured noise levels⁵ varied as wind speed to the 3.65 power, $U^{3.65}$. This result was also confirmed by Perrone's⁸ measurement in the Atlantic Ocean. At frequencies above 200 Hz, the wind speed dependencies of the analytically derived source levels and relevant measured noise levels⁴ were directly proportional to the so-called "whitecap index," $R(U)$. The whitecap index is defined as the percent

of the ocean surface covered by whitecaps and streaks and varies as a function of wind speed (in knots) as

$$R(U) = \begin{cases} 0 & 0 \text{ kts} \leq U < 9 \text{ kts} \\ \frac{U^3}{1749.60} - \frac{U^2}{81.00} + \frac{U}{4.32} - 1.5 & 9 \text{ kts} \leq U < 30 \text{ kts} \\ R(30)(U/30)^{1.5} & U \geq 30 \text{ kts} \end{cases} \quad (2)$$

Since the onset of whitecaps occurs for wind-speeds of 9 knots, $R(U)$ was taken to be zero below 9 knots. For the wind speed interval between 9 and 30 knots, $R(U)$ was empirically fit to experimental measurements,⁹ and above 30 knots the saturation of $R(U)$ was taken into account using Perrone's data.⁸ This saturation effect was not considered in the author's latest published analyses.⁴

The frequency dependence of the wind-generated source level was relatively flat from 10 to 1000 Hz where turbulent pressure fluctuations in the atmosphere and the impact of ocean spray and streaks were dominant physical mechanisms. A negative slope is predicted from 5 to 10 Hz where wave-wave interaction is the dominant physical mechanism. The measured data^{5,6} show a relatively flat spectrum above 10 Hz, but there is no data available to validate the negative slope predicted from 5 to 10 Hz.

The source level densities presented in Figure 1 are only a first estimate of the wind-generated source levels that are consistent with the appropriate measured data. Many further analytical developments and appropriate measurements are necessary to refine and completely validate

wind-generated source levels. The source levels shown in Figure 1 are substantially different than the Wenz curves¹ because the former is an estimation of source level while the latter is an estimation of the noise level. The Wilson source level curves are intended for use with an appropriate transmission loss model to estimate ambient noise levels.

3.0 DEVELOPMENT OF WIND-GENERATED NOISE MODEL

The wind-generated source level densities presented in the previous section need to be combined with an appropriate transmission loss model in order to estimate ambient noise levels. ASTRAL¹⁰ was selected because it is currently being used in the model to estimate shipping noise, and because ASTRAL's range averaging property is very compatible with a source such as wind, which is distributed over large ocean areas.

In any ambient noise model that includes both wind and shipping, it is efficient to treat both noise sources alike when applying the transmission loss model. To accomplish this objective, the concept of a "Wind Equivalent Ship" (WES) was developed. Since the model computes ship noise from shipping densities in 1° x 1° Latitude/Longitude cells, wind source level densities were calculated for the same 1° x 1° cells. This was done simply by multiplying the area (A_i yd²) of the i th 1° x 1° cell

$$A_i = 8.25 \times 10^{11} (\cos L_l - \cos L_u) \quad (3)$$

(where L_l and L_u are the latitudes in the $1^\circ \times 1^\circ$ cell nearest to and farthest from the equator, respectively) by the source level density from Table I, $SL(U_i, f)$, for the frequency of interest and for the average wind speed, U_i , over the i^{th} cell:

$$\overline{SL}(U_i, f) = SL(U_i, f) A_i \quad (4)$$

The source level, $SL(U_i, f)$, is equivalent to a ship of the same source level located at the center of the $1^\circ \times 1^\circ$ cell. One important difference between a ship and the WES of the same source level remains: source depth. Wind is a near surface source while ships radiate noise from a point well below the surface (a 20-ft ship source depth is assumed in the model). However, since the wind source directivity is believed to be dipole in nature, its source depth can be lowered to depth, z , below the ocean surface by

$$\overline{\overline{SL}}(U_i, f, z) = \frac{\overline{SL}(U_i, f, z=0)}{4k^2z^2} \quad (5)$$

where k is the acoustic wave number. As shown in the appendix, the term $4k^2z^2$ accounts for surface image interference for $kz \sin \theta \ll 1$.

To compute the ambient noise from the i^{th} cell as measured by a receiver at depth d , the transmission loss is computed between the source coordinates (source location

and depth) and receiver coordinates (receiver, location and depth) at the frequency of interest. The noise from the i^{th} cell is

$$N_i = TL_i \overline{SL}(U_i, f, z) \quad (6)$$

The shipping noise is computed similarly and added to the wind noise and only one transmission loss computation is made for the i^{th} cell. By including only cells from a given azimuthal sector, the model can estimate the noise arriving from only that sector. By making the sector small, the noise horizontal directionality can be estimated from all sectors from 0° T to 360° T. If the measuring apparatus is an array, the beam pattern can be convolved with the sector noise estimates to estimate beam noise. Or, if all the sectors are added together, the omnidirectional noise can be estimated. Wind noise and shipping noise can also be computed separately. Cells that are split between two sections have their wind and shipping source levels split between the sectors proportional to the area split.

The above procedure is currently followed for cells greater than 50 nm from the measurement site. The resolution of the transmission loss model is not good enough for the nearby cells, and the local wind noise levels are taken from Figure 1 directly and added to the distant noise.

4.0 MODEL/DATA COMPARISON

ACODAC data collected over a 10 day period in September 1973 from 3 hydrophones (696m, 4055m, and 5521m)

located near 39°N Latitude/143°W Longitude are used in the model/data comparison. Time series and 10 day averages of spectrum levels were computed at 12.5, 25, 50, 100, 160 and 250 Hz. Sound channel axis depth, critical depth, and water depth are 655m, 3860m, and 5555m respectively. The average local wind speed-for the 10 day period was 20 knots and there were no major distant storms during this period.

Figure 2 shows a comparison of model estimates with 10 day average spectrum levels at five frequencies and three receiver depths throughout the water column. Shipping noise was dominant for the upper two receivers (696m and 4055m) below 100 Hz. Wind noise was dominant for these receivers at 160 Hz and 250 Hz. The model estimates for the near bottom receiver (5521m) are plotted in Figure 2 for wind only, shipping only, and total noise. Wind noise is dominant throughout the spectrum, especially above 100 Hz. Notice the flat spectra characteristic of wind noise in both the model estimates and measured data. The model/data comparisons shown in Figure 2 are very good, in the author's opinion, and show that the model does well for long time averages. How the model estimates compare with the noise time series is discussed next.

The time series for the middle hydrophone (4055m) at 250 Hz is plotted every 12 hours in Figure 3. If a nearby ship or ship tow source operations were present a range of values is plotted. For example, on 18 September 1973 a nearby ship was seen in the 250 Hz time series and the noise level increased from 66 dB/ $\mu\text{Pa}/\text{Hz}^{1/2}$ to 69 dB/ $\mu\text{Pa}/\text{Hz}^{1/2}$ during the passage of this ship. This

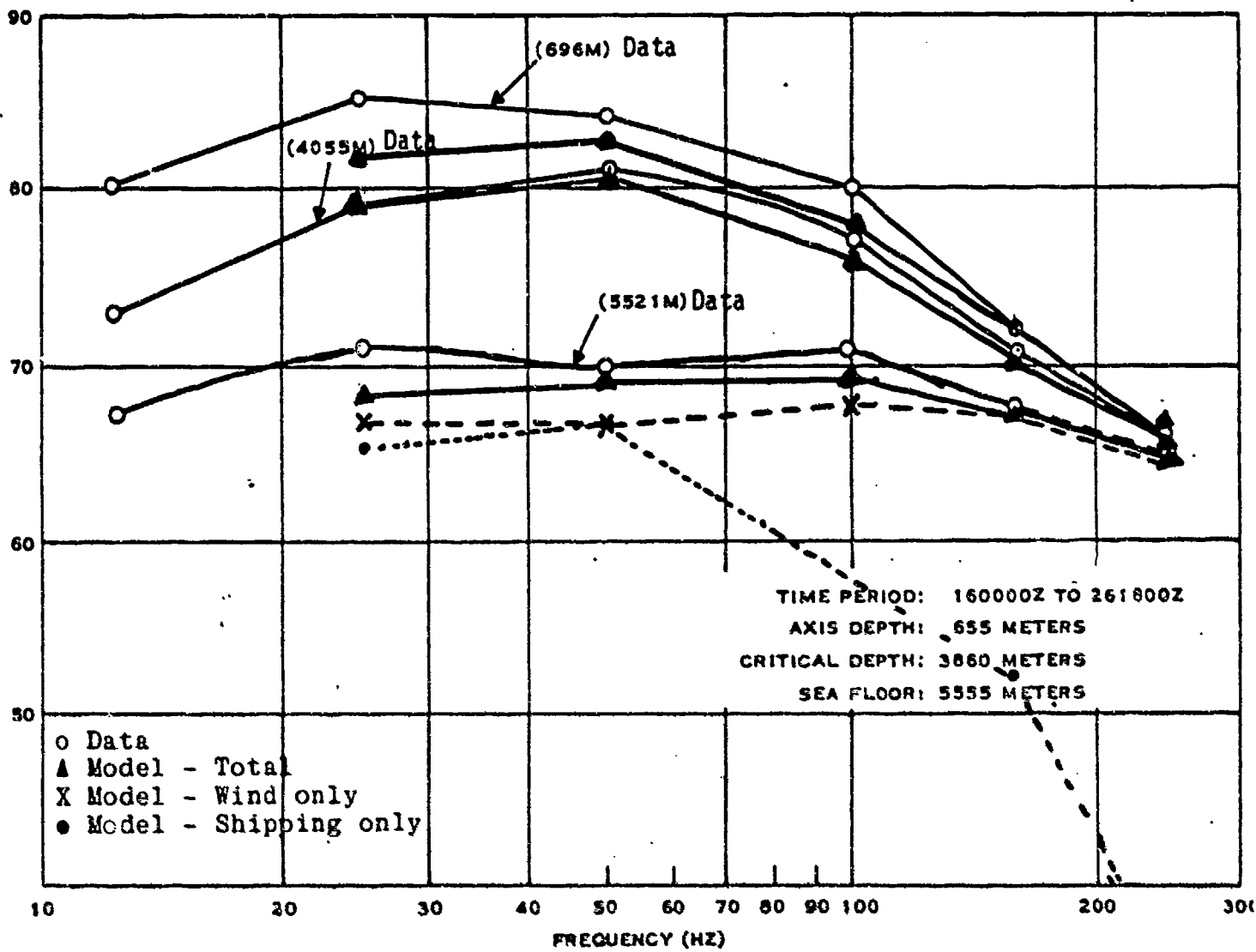


Figure 2. Model/Data Comparison - 10 Day Averages

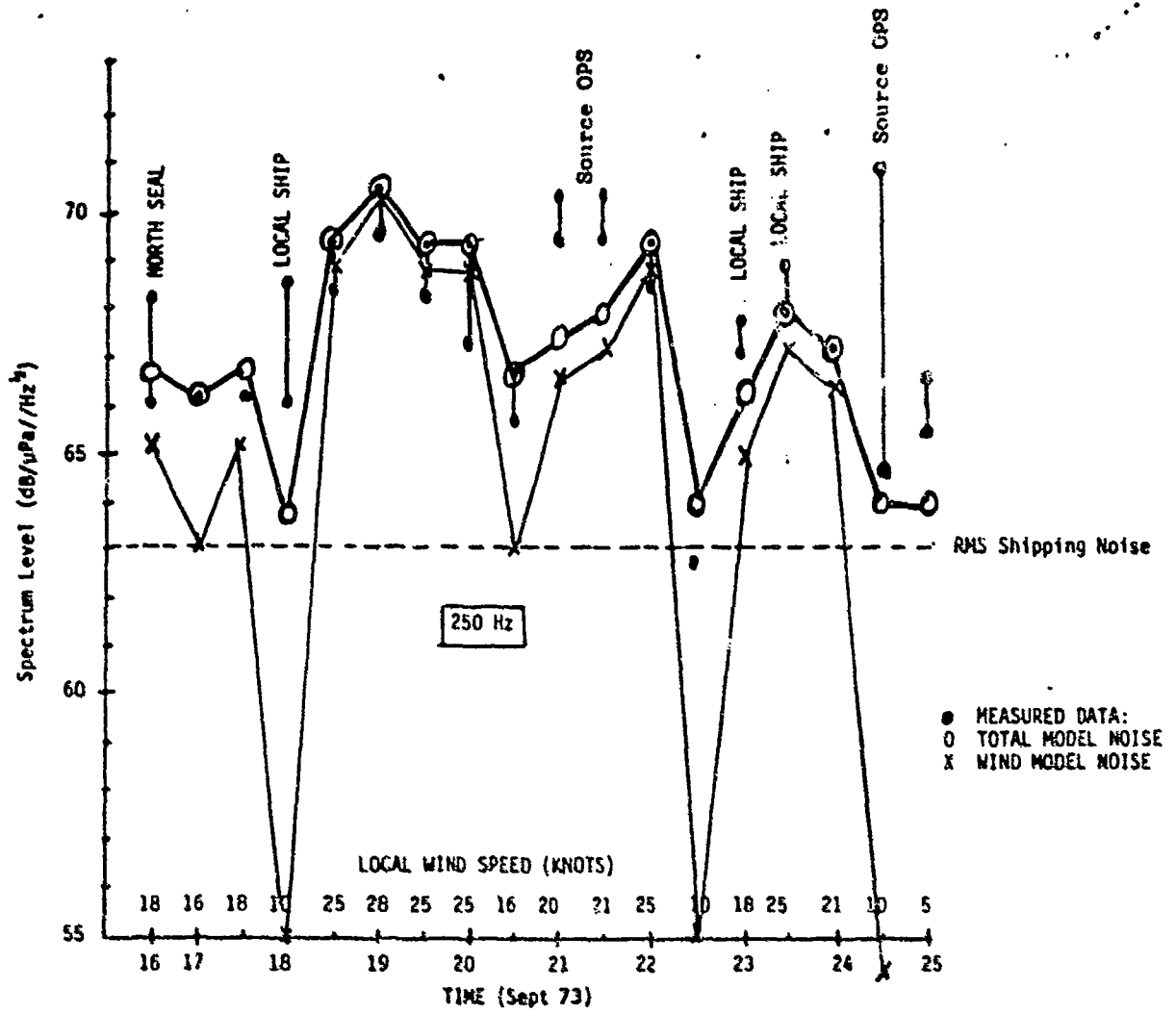


Figure 3 Model/Data Comparison at 250Hz - Time Series

range of values is plotted on Figure 3. The local wind speed for each 12 hour period is specified along the time axis of Figure 3 and the model wind noise estimates are plotted throughout this period. The model estimate of historical shipping noise does not change during this period since the model shipping densities and model transmission loss is constant. The model estimates of total noise (wind plus shipping) is plotted and compares very favorably with the measured data for this 10 day period.

5.0 CONCLUSIONS

This preliminary evaluation of the wind noise model (and, thus, the source level densities given in Figure 1 and Table I) shows very good agreement between model and data, in the author's opinion. However, a much more extensive evaluation for different receiver locations and larger storms needs to be performed. This preliminary evaluation is only intended to be a start in the right direction in modeling storm noise.

Appendix
RELATIONSHIP BETWEEN NOISE LEVEL AND SOURCE LEVEL

In deriving the source level densities in Figure 1, great care was taken to address the difference between noise level and source level. In order to validate wind-generated noise source levels with measured noise levels, only a very select set of measured data can be considered. It is shown⁷ below that source level and noise level are related by a constant factor only when the noise measurements are taken well below critical depth near a region with a poor reflecting bottom where only the noise from the near vertical sea surface above the hydrophone is measured. In this case, the relationship between source level and noise level for a dipole radiation pattern is given by

$$NL(f,U) = \pi SL(f,U) \quad (A-1)$$

Assuming that only direct paths are important for sea surface above a very deep receiver, the noise level, NL, and source level, SL, are related by

$$NL = \int_{\text{Ocean Surface}} SL(\theta_0) \cdot TL(\theta_0, \theta_r) dA \quad (A-2)$$

where the transmission loss is given by

$$TL(\theta_0, \theta_r) = \frac{\cos \theta_0}{R \sin \theta_r \frac{dR}{d\theta_0}} \quad (A-3)$$

and where the ocean surface incremental area is given by

$$dA = R dR d\phi \quad (A-4)$$

In Equations (A-2), (A-3) and (A-4), the variables are defined as follows:

- θ_0 = surface source angle
- θ_r = receiver arrival angle
- R = horizontal source/receiver range
- ϕ = azimuth angle
- A = ocean surface area

Substituting Equations (A-3) and (A-4) into Equation (A-1) and integrating over azimuth yields

$$NL = 2\pi \int_{\theta_0^{\min}}^{90^\circ} \frac{SL(\theta_0) \cos(\theta_0) d\theta_0}{\sqrt{1 - (C_r/C_0)^2 \cos^2 \theta_0}} \quad (A-5)$$

where

$$\cos \theta_r = \frac{C_r}{C_0} \cos \theta_0 \quad (A-6)$$

with C_r and C_0 being the sound speed at the receiver and surface respectively. For the purpose of the analysis, a homogenous ($C_r = C_0$) medium will be assumed and for a "sine power" source, $SL(\theta_0) = SL(\sin^m \theta_0)$, Equation (A-6)

$$NL = \frac{2 \pi SL}{m} \quad (A-7)$$

For a dipole source ($m=2$), Equation (A-7) becomes

$$SL = \frac{NL}{\pi} \quad (A-8)$$

Equation (A-8) is the connection between the noise levels plotted in Figure 1 and the source levels listed in Table I.

If computing efficiency was not of concern, Equation (A-8) could be used as the final relationship between source level and noise level. However, ASTRAL transmission loss is currently computed for shipping in the model for a source depth of 20 feet. In order to avoid another computation of transmission loss for the wind surface ($z=0$) source, the following source depth relation is used

$$TL(z) = TL(z=0) + \sin^2(kz \sin \theta_0) \quad (A-9)$$

and

$$\text{for } kz \sin \theta \ll 1$$

$$(\sin^2 \theta_0) TL(z=0) = \frac{TL(z)}{4k^2 z^2} \quad (A-10)$$

The approximation in going from Equation (A-9) to (A-10) is valid for long distance (small angles, θ_0), low frequency

calculations. For example, for $f = 150$ Hz (or $\lambda \approx 32.5$ ft and $k = 0.193$ ft⁻¹) and for $z = 20$ ft, the restriction on source angle is

$$\theta_0 \ll 15^\circ, \quad (\text{A-11})$$

which is a good approximation for long range propagation. Below 150 Hz, the approximation gets better, and Equation (A-10) shows that a surface dipole can be approximated by a monopole source at depth z whenever $kz \sin \theta_0 \ll 1$.

REFERENCES

1. Wenz, G.M., "Ambient Noise in the Ocean: Spectra and Sources," J. Acoust. Soc. Am., 48:362, 1970.
2. Ross, D., J. Mahler, and L. Solomon, "Navy Interim Shipping Distribution," Unpublished Report.
3. Wilson, J.H., "Very Low Frequency (VLF) Wind-Generated Noise Produced by Turbulent Pressure Fluctuations in the Atmosphere Near the Ocean Surface," J. Acoust. Soc. Am. 66 (5), Nov. 1979.
4. Wilson, J.H., "Low Frequency Wind-Generated Noise Produced by the Impact of Spray with the Ocean's Surface," J. Acoust. Soc. Am., to be published.
5. Wittenborn, A. and J. Shooter, "Ambient Noise and Associated Propagation Factors as a Function of Depth and Wind Speed in the Deep Ocean," to be published.
6. Morris, G.B., "Depth Dependence of Ambient Noise in the Northeastern Pacific Ocean," J. Acoust. Soc. Am. 64, 581-590, 1978.
7. Spofford, C., SAI private communication.
8. Perrone, A.J., "Ambient-Noise Spectrum Levels as a Function of Water Depth," J. Acoust. Soc. Am., 48:632, 1970.
9. Ross, D.B. and Cardone, B., "Observations of Oceanic Whitecaps and their Relation to Remote Measurements of Surface Wind Speed," J. Geophys. Rev. 79, 444-452 (1974).
10. Spofford, C.W. and L.S. Blumen, "The ASTRAL Model, Volumes I and II," Science Applications, Inc. Technical Report, March 1978.



DEPARTMENT OF THE NAVY

OFFICE OF NAVAL RESEARCH
875 NORTH RANDOLPH STREET
SUITE 1425
ARLINGTON VA 22203-1995

IN REPLY REFER TO:

5510/1
Ser 321OA/011/06
31 Jan 06

MEMORANDUM FOR DISTRIBUTION LIST

Subj: DECLASSIFICATION OF LONG RANGE ACOUSTIC PROPAGATION PROJECT
(LRAPP) DOCUMENTS

Ref: (a) SECNAVINST 5510.36

Encl: (1) List of DECLASSIFIED LRAPP Documents

1. In accordance with reference (a), a declassification review has been conducted on a number of classified LRAPP documents.
2. The LRAPP documents listed in enclosure (1) have been downgraded to UNCLASSIFIED and have been approved for public release. These documents should be remarked as follows:

Classification changed to UNCLASSIFIED by authority of the Chief of Naval Operations (N772) letter N772A/6U875630, 20 January 2006.

DISTRIBUTION STATEMENT A: Approved for Public Release; Distribution is unlimited.

3. Questions may be directed to the undersigned on (703) 696-4619, DSN 426-4619.

A handwritten signature in black ink that reads "B. F. Link".

BRIAN LINK
By direction

Subj: DECLASSIFICATION OF LONG RANGE ACOUSTIC PROPAGATION PROJECT
(LRAPP) DOCUMENTS

DISTRIBUTION LIST:

NAVOCEANO (Code N121LC – Jaime Ratliff)
NRL Washington (Code 5596.3 – Mary Templeman)
PEO LMW Det San Diego (PMS 181)
DTIC-OCQ (Larry Downing)
ARL, U of Texas
Blue Sea Corporation (Dr. Roy Gaul)
ONR 32B (CAPT Paul Stewart)
ONR 321OA (Dr. Ellen Livingston)
APL, U of Washington
APL, Johns Hopkins University
ARL, Penn State University
MPL of Scripps Institution of Oceanography
WHOI
NAVSEA
NAVAIR
NUWC
SAIC

Declassified LRAPP Documents

Report Number	Personal Author	Title	Publication Source (Originator)	Pub. Date	Current Availability	Class.
Unavailable	Unavailable	SELF-TENSIONING ACOUSTICAL HORIZONTAL LINE ARRAY (SPRAY) DATA ANALYSIS. FINAL REPORT OF BEARING STAKE TESTS JANUARY THRU MARCH 1977.	Sanders Associates, Inc.	790109	ADC017579	U
ARL TR 7924	Mitchell, S. K., et al.	VOLUME IVB. DATA POINTS 10, 11 AND 12 RAW DATA ANALYSIS OF ACOUSTIC BOTTOM INTERACTION IN BEARING STAKE (U)	University of Texas, Applied Research Laboratories	790223	ADE001369; NS; ND	U
TTU1886502F	Eichenberger, D.	REPORT FOR CHURCH STROKE II OCEANOGRAPHIC SERVICES	Texas Instruments, Inc.	790326	ADB036751; ND	U
Unavailable	Unavailable	FINAL REPORT, 1 NOVEMBER 1976-31 DECEMBER 1978	Xonics, Inc.	790430	ADB037987	U
Unavailable	Mitchell, T. M.	PREMOBILIZATION OF R/V INDIAN SEAL	Texas Instruments, Inc.	790531	ADB039703	U
Unavailable	Hays, E. E.	ACODAC AMBIENT NOISE PROGRAM	Woods Hole Oceanographic Institution	790601	ADB040404	U
LRAPPR 79029	Unavailable	INTRODUCTION TO THE LRAPP ENVIRONMENTAL-ACOUSTIC DATA BANK (U)	Naval Ocean R&D Activity	790601	ADB041066; NS	U
USRD NO. 4807	Unavailable	MEASUREMENTS ON AQUADYNE MODEL AQ-1 ELEMENTS FOR THE UPGRADED LAMBDA ARRAY	Naval Research Laboratory	790802	ND	U
Unavailable	Ellis, G. E.	SUMMARY OF ENVIRONMENTAL ACOUSTIC DATA ANALYSIS	University of Texas, Applied Research Laboratories	790814	ADA073876	U
BR U0048-9C2	Unavailable	TAP III FINAL REPORT (U)	Bunker-Ramo Corp. Electronic Systems Division	790901	ND	U
ORITR1245	Moses, E. J.	OPTIONS, REQUIREMENTS, AND RECOMMENDATIONS FOR AN LRAPP ACOUSTIC ARRAY PERFORMANCE MODEL (U)	ORI, Inc.	790917	NS; ND	U
Unavailable	Colborn, J. G., et al.	EVALUATION OF STANDARD OCEAN CANDIDATES	Pacific-Sierra Research Corp.	800301	ADA087304	U
Unavailable	Kirby, W. D.	ENVIRONMENTAL ACOUSTIC SUPPORT FOR FLEET OPERATIONS AND NATO	Science Applications, Inc.	801112	ADB052623	U
Unavailable	Unavailable	SUMMARY OF ENVIRONMENTAL ACOUSTIC MEASUREMENTS, MODELING AND ANALYSIS	University of Texas, Applied Research Laboratories	801215	ADB053770	U
Unavailable	Renner, W. W., et al.	SURFACE DUCT, ROUGH SURFACE SCATTERING, AND CUSPED CAUSTIC IMPROVEMENTS FOR FACT	Science Applications, Inc.	810301	ADA126250	U
Unavailable	Wilson, J. H.	WIND-GENERATED NOISE MODELING	Science Applications, Inc.	810401	ADA190143	U
Unavailable	Goit, E. H.	TOWED ARRAY PERFORMANCE PREDICTION SYSTEM - VERSION 1.2	Science Applications, Inc.	810701	ADB059397	U
3	Unavailable	FINAL REPORT	University of Texas, Applied Research Laboratories	810721	ND	U